The Effect of TiO_2 Addition on the Characteristics of $CuFe_2O_4$ Ceramics for NTC Thermistors

Wiendartun 1, Dani Gustaman Syarif 2
1 Department of Physics, UPI, Jl. Setiabudhi, Bandung, e-mail: wien@upi.edu
2 Nuclear Technology Center of Materials and Radiometry – BATAN, Jl. Tamansari 71, Bandung 40132.
Telp. 62-22-2503997, Fax.: 62-22-2504081, e-mail: danigusta@yahoo.com

Abstract.

The effect of TiO_2 addition on the characteristics of $CuFe_2O_4$ ceramics for NTC thermistors has been studied. This study was to get an alternative NTC thermistor ceramic from $CuFe_2O_4$ based-one. The ceramics were produced by pressing a homogeneous mixture of CuO, Fe_3O_4 and TiO_2 (0, 0.25 and 0.75 w/o) powders in appropriate proportions to produce $CuFe_2O_4$ based ceramics and sintering the pressed powder at 1100^{o}C for 2 hours in air. Electrical characterization was done by measuring electrical resistivity of the ceramics at various temperatures (25^{o}C-100^{o}C). Microstructure and structural analyses were also carried out by using optical microscopy and x-ray diffraction (XRD), respectively. The XRD analyses showed that the $CuFe_2O_4$ ceramic with and without TiO_2 addition are composed of two crystal structures i.e. cubic and tetragonal spinels. Microstructural data showed that all of the ceramics contain rounded grains and the second phase was segregated at grain boundaries. According to the electrical data, it was known that the TiO_2 addition increased the thermistor constant (B) and the room temperature electrical resistivity (ρ_{RT}). The value of B and ρ_{RT} of the produced $CuFe_2O_4$ ceramics fitted those for market requirement.

Key words: *Thermistor, NTC, $CuFe_2O_4$, TiO_2.*

I. INTRODUCTION

The NTC thermistors are widely used in the world due to their potential use in many sectors, 1) for many applications such as temperature measurement, circuit compensation, suppression of in rush-current, flow rate sensor and pressure sensor, 1), 2). It is well known that most NTC thermistors are produced from spinel ceramics based on transition metal oxides with general formula of AB_2O_4 where A is metal ion in tetrahedral position and B is metal ions in octahedral position, 3)-10). Many studies have been done to improve the characteristics of the spinel based-NTC thermistors, 6), 7), 11). However, the study on the effect of TiO_2 addition on the characteristics of $CuFe_2O_4$ spinel ceramics sintered at 1100^{o}C for NTC thermistor has not been reported yet.

Many reports show that the $CuFe_2O_4$ ceramics can be applied as soft magnet, 12)-14) and catalyst, 15)-17), however, potentially; the $CuFe_2O_4$ ceramics have capability of being NTC thermistors too due to its semi conductive property. This ceramic is economically interesting because it may be produced using local abundant mineral, such as hematite and magnetite as a part of raw material. According to CuO-Fe_2O_3 phase diagram, 18), there is an area where the ceramic composing of CuO and Fe_2O_3 heated at 1100^{o}C will have a microstructure containing liquid phase. In room temperature, the liquid phase will be a boundary material. This boundary material theoretically may affect the characteristics of the ceramics, especially the electrical characteristics. Since an additive of TiO_2 is added, the characteristics of the $CuFe_2O_4$ may change because two conditions may occur since the TiO_2 is added to the $CuFe_2O_4$. The conditions are the TiO_2 dissolves in the $CuFe_2O_4$ by substituting Cu ions or Fe ions (first) and the TiO_2 does not dissolve but segregated at grain boundaries and may react with the liquid phase that originally exists (second).

Since the first condition occurs, the $CuFe_2O_4$ ceramics may have a lower electrical resistivity when the substitution of Fe^{3+} and /or Cu^{2+} by Ti^{4+} ions creates free electron in the conduction band. Meanwhile, since the second one occurs, the electrical resistivity may be higher because the segregated TiO_2 may change the microstructure. This works is to know the effect of TiO_2 addition on the characteristics of the $CuFe_2O_4$ ceramics for NTC thermistors, especially the electrical characteristic based on the above-mentioned hypothesis.

II. METHODOLOGY

Powders of CuO, Fe_3O_4 and TiO_2 were weighed in appropriate proportions to fabricate TiO_2 added-$CuFe_2O_4$ ceramics where the TiO_2 were 0, 0.25 and 0.75 w/o (weight %) and mechanically mixed. The mixture of powders was calcined at 800^{o}C for 2 hours. After calcination, the powder was crushed and sieved with a siever of < 38 μm. The sieved powder was then pressed with pressure of 3,9 ton/cm^2 into green pellets. The green pellets were sintered at 1100^{o}C for 2 hours in air with heating and cooling rates of 6^{o}C/minutes.

The crystal structure of the sintered pellets was analyzed with x-ray diffraction (XRD) using Kα radiation at 40KV and 30mA. The microstructure of the pellets was investigated by an optical microscope. Before optical investigation, the pellets were ground, polished, and etched. The opposite-side surfaces of the sintered pellets were coated with Ag paste. After the paste was dried at room temperature, the Ag coated-pellets were heated at 500°C for 10 minutes. The resistivity measurement was performed at various temperatures from 25°C to 100°C in steps of 5°C.

III. RESULTS

Fig.1, Fig.2, and Fig.3 show the XRD profile of $CuFe_2O_4$ ceramics added with 0, 0.25 and 0.75 w/o TiO_2, respectively. The pattern of Fig.1 contains peaks of cubic $CuFe_2O_4$ but at $2\theta = 53.6^o$ there is a peak of tetragonal one (after being compared to the XRD standard profile of cubic $CuFe_2O_4$ from JCPDS No. 25-0283 and of tetragonal $CuFe_2O_4$ from JCPDS No. 34-0425). The coexistence of cubic and tetragonal phases is clearly shown in Fig. 2 and Fig. 3. This feature suggests that the cooling rate during sintering was high enough (fast cooling). Goya and Rechenberg, 19) showed that $CuFe_2O_4$ crystallized to tetragonal spinel when it was cooled slowly from a high temperature. The feature of Fig. 2 and Fig. 3 shows that there is an effect of TiO_2 addition. The structure of the ceramics added with 0.25 w/o and 0.75 w/o is composed of two structures of cubic and tetragonal spinels. The effect seems to be complex as indicated by Fig. 3 that shows that at a high concentration of TiO_2 the ratio of cubic to tetragonal becomes higher (Bragg peak of 311 of cubic becomes higher than that of 211 tetragonal). However, it can be noticed that the addition of TiO_2 decreases the cooling rate.

There is an additional peak at 2θ about 40 (S) in the XRD pattern of $CuFe_2O_4$ ceramic without addition of TiO_2. This peak comes from a second phase. It may be the grain boundary material that melted during sintering. Compared to the pattern of standard CuO (JCPDS No. 05-0661), it is known that the additional peak (S) is the peak of CuO (200). The same peak and other additional peak cannot be observed in all TiO_2 added samples. It may be because, if any, the yield of the reaction between TiO_2 and CuO (original melted material) is in small concentration and may be due to the small concentration of added TiO_2 that is smaller that the precision limit of the x-ray diffractometer used. According to ionic radii data, there is a possibility that a part of the added TiO_2 dissolved in the $CuFe_2O_4$ spinel ceramic but it cannot be concluded from the XRD profiles in this works. The microstructure and electrical data may be used to evaluate whether a part of the TiO_2 added was dissolved or not.

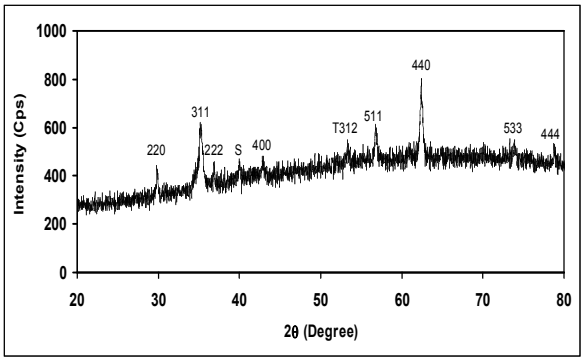

Fig. 1. XRD profile of $CuFe_2O_4$ ceramic without TiO_2 (T means peak from tetragonal and S is peak from second phase).

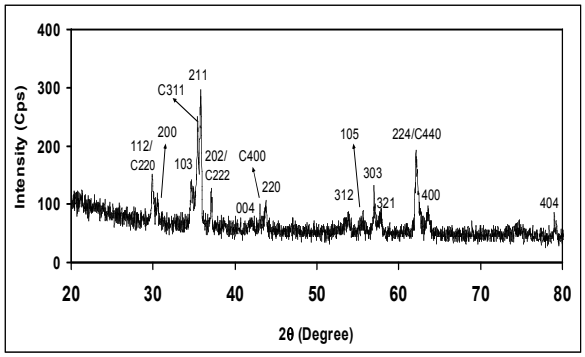

Fig. 2. XRD profile of 0.25 w/o TiO_2 added-$CuFe_2O_4$ Ceramic (C means peak from cubic).

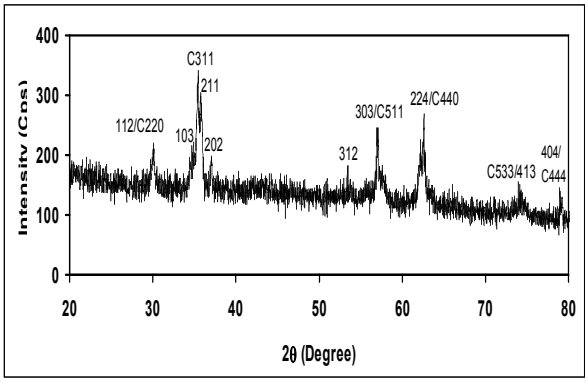

Fig. 3. XRD profile of 0.75 w/o TiO_2 added-$CuFe_2O_4$ Ceramic (C means peak from cubic).

Fig.4, Fig.5 and Fig. 6 are microstructures of the $CuFe_2O_4$ ceramics added with 0, 0.25 and 0.75 w/o TiO_2, respectively.

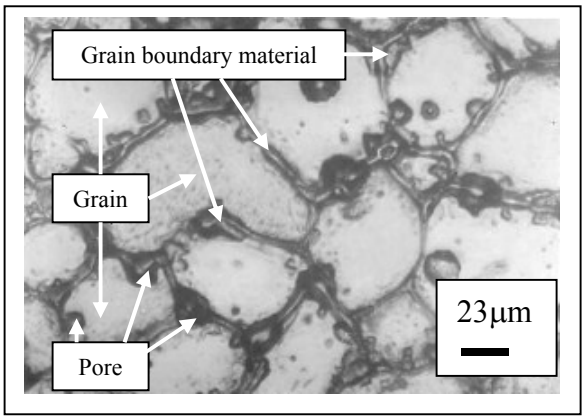

Fig. 4. Microstructure of the $CuFe_2O_4$ ceramic without TiO_2.

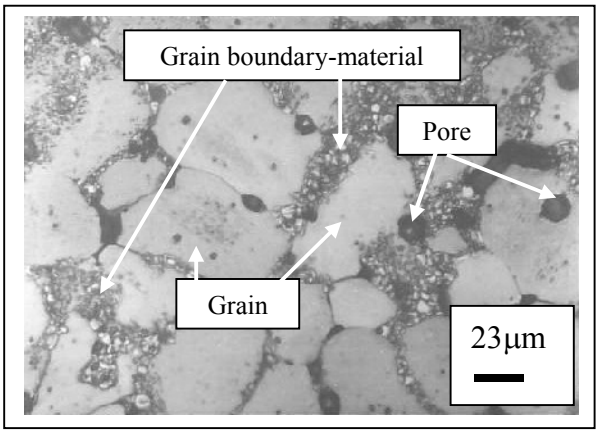

Fig. 5. Microstructure of the 0.25 w% TiO_2 added-$CuFe_2O_4$ ceramic.

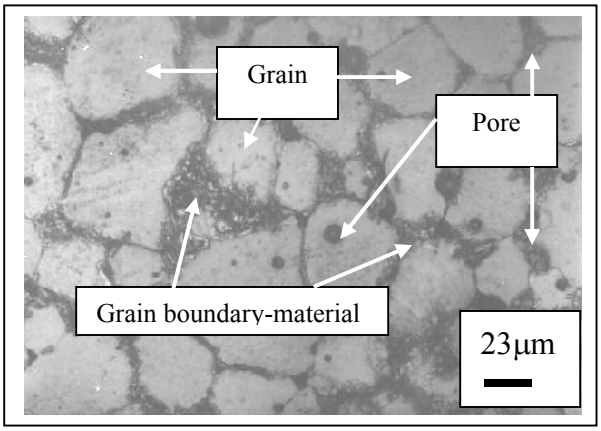

Fig. 6. Microstructure of the 0.75 w/o TiO_2 added-$CuFe_2O_4$ ceramic.

It is clearly seen that all ceramics have rounded grains, suggesting the present of liquid phase during sintering. The grains are relatively large, as the consequence of the liquid phase sintering. Based on CuO-Fe_2O_3 phase diagram, 18), the liquid phase is about 15 % of the ceramics. This amount is considerable and affected the grain growth during sintering significantly. This is the reason of large grain formation found. From Fig. 5, Fig. 6 and Fig. 7 it can be seen that the addition of TiO_2 decreases the grain size though it is not significant. It is can be seen also from those figures that the appearance of grain boundary material for the ceramic with and without TiO_2 is different, suggesting the different material. The grain material in the $CuFe_2O_4$ ceramic without TiO_2 addition is CuO, but that in the $CuFe_2O_4$ ceramic with TiO_2 addition may be reaction product of CuO and TiO_2 or other material. However, the absent of the additional peaks in the XRD patterns of TiO_2 added-samples may indicate that the main grain boundary material is the same structure with the matrix.

The electrical data of the TiO_2 added-$CuFe_2O_4$ ceramics is shown in Fig.7 and Table 1.

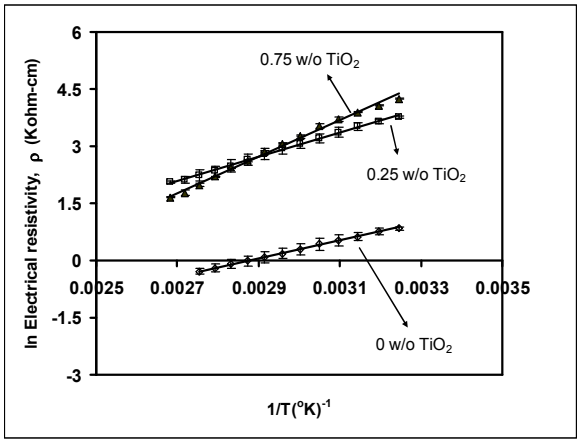

Fig. 7. Ln resistivity (ρ) vs. 1/T of TiO_2 added-$CuFe_2O_4$ ceramics.

The electrical data of Fig. 7 shows that the electrical characteristics of the ceramics follow the NTC tendency expressed by eq. 1. As shown in Table 1, the addition of TiO_2 increases the room temperature resistivity (ρ_{RT}) and thermistor constant (B). Compared to the (B) value for market requirement where $B \geq 2000^oK$, the value of B for our ceramics is larger and it means that our ceramics are better.

$$\rho = \rho_o \exp. (B/T) \text{ .....(1)}$$

where, ρ = Electrical resistivity, ρ_o = Electrical resistivity at infinite temperature, B is the thermistor constant and T is the temperature in Kelvin.

Table 1. Electrical characteristics of the TiO_2 added-$CuFe_2O_4$ ceramics.

No.	Additive of TiO_2 (w/o)	B (^oK)	α (%/^oK)	ρ_{RT} (Kohm-cm)
1.	0	2350	2.61	2.9
2.	0.25	3187	3.54	60.5
3.	0.75	4759	5.29	119.9

IV. DISCUSSION

The rounded grains of the ceramics are caused by melted material at the grains boundaries. According to the CuO-Fe_2O_3 phase diagram, 18), the melted material contained by the $CuFe_2O_3$ without TiO_2 addition is about 15 mole %. This is a relatively large amount. This large amount of melted material considerably promoted grain growth during sintering. This is the reason of the large grains formation found in our ceramics. In the samples containing TiO_2, the TiO_2 may dissolve or segregate. Since there is no interaction between the original melted material and the TiO_2, and the TiO_2 is dissolved in the $CuFe_2O_4$ ceramic by substituting Fe^{+3} or Cu^{2+} following eq. 2 or 3, the electrical resistivity of the ceramic should be lower, and the microstructure will the same with that of the $CuFe_2O_4$ ceramic. The feature of the grain boundary material in the samples added with TiO_2 (See Fig. 5 and 6) is different than that of the ceramic without TiO_2 addition (See Fig. 4). This indicates that the added TiO_2 is likely to segregate at grain boundaries. The segregated TiO_2 may react with the original melted material but it cannot be known from the XRD profile. The segregated TiO_2 then inhibits the grain growth during sintering. This feature is in agreement with the data of microstructure showing that the grain size slightly decreases following the increase of the added TiO_2. The thickness of the grain boundary material found in $CuFe_2O_4$ ceramic (without TiO_2) is relatively thinner than the thickness of the grain boundary material found in those containing TiO_2. This is a factor that may affect the electrical characteristics of the ceramics.

The change of the electrical characteristics is controlled by the change of the microstructure that may change by the TiO_2 addition. Since the added-TiO_2 dissolved in $CuFe_2O_4$ by substituting Cu and/or Fe following eq. 2 and 3, the room temperature resistivity (ρ_{RT}) and thermistor constant (B) should decrease. The increase (ρ_{RT}) and (B) as shown by our data indicates that the added TiO_2 is not dissolved in the $CuFe_2O_4$ and tends to segregate at the grain boundaries. The increase of the (ρ_{RT}) and (B) is mainly caused by decrease of grain size and the change of the feature of the grain boundary material. The ceramics containing small grains and much grain boundary material contains large grain boundary area.. Because the grain boundaries act as a scattering center of charge carriers, the relative frequency of electron scattering increases, resulting in an increase in the room temperature resistivity and thermistor constant.

$$2TiO_2 = 2Ti^{+}_{Fe} + 3O_O + \tfrac{1}{2}\, O_2(gas) + 2e \quad (2)$$

$$TiO_2 = Ti^{2+}_{Cu} + O_O + \tfrac{1}{2}\, O_2\,(gas) + 2e \quad \ldots(3)$$

where, Ti^{+}_{Fe} = Ti^{4+} ion occupies Fe sublattice, Ti^{2+}_{Cu} = Ti^{4+} ion occupies Cu sublattice, O_O = Oxygen ion occupies oxygen sublattice, O_2(gas) = Released oxygen gas and e = Released electron.

V. CONCLUSION

The $CuFe_2O_4$ ceramic can be applied as NTC thermistor. The grain size of the $CuFe_2O_4$ ceramics decreases by addition of TiO_2 because the added TiO_2 is segregated and co-exists with the melted material at grain boundaries and inhibits grain growth during sintering. The addition of TiO_2 increases the room temperature resistivity (ρ_{RT}) and the thermistor constant (B) as well as the sensitivity (α) of the $CuFe_2O_4$ ceramics by changing the microstructure. The value of (ρ_{RT}), (B) and (α) of the $CuFe_2O_4$ ceramics made in this work fits the market requirement.

ACKNOWLEDGMENT

The authors are grateful to DIKTI, Department of National Education of Indonesian Government for financial support under HIBAH PEKERTI program with contract No. 014/SPP/PP/DP2M/II/2006.

VI. REFERENCES

1. BetaTHERM Sensors [on line]. Available: http://www.betatherm.com.
2. Eun Sang Na, Un Gyu paik, Sung Churl Choi, Journal of Ceramic Processing Research, Vol.2, No. 1, pp 31-34, (2001).
3. Yoshihiro Matsuo, Takuoki Hata, Takayuki Kuroda, US Patent 4,324,702, April 13, (1982).
4. Hyung J. Jung, Sang O. Yoon, Ki Y. Hong, Jeon K. Lee, US Patent 5,246,628, September 21, (1993).
5. Kazuyuki Hamada, Hiroshi Oda, US Patent 6,270,693, August 7, (2001).
6. Eun Sang Na, Un Gyu paik, Sung Churl Choi,

Journal of Ceramic Processing Research 2 (1), 31 (2001).
7. K. Park, Materials Science and Engineering, B104, 9 (2003).
8. K. Park, D.Y. Bang, Journal of Materials Science: Materials in Electronics 14, 81 (2003).
9. Shopie Gulemet Fritsch, Jaouad Salmi, Joseph Sarrias, Abel Rousset, Shopie Schuurman, Andre Lannoo, Materials Research Bulletin 39, 1957 (2004).
10. R. Schmidt, A. Basu, A.W. Brinkman, Journal of The European Ceramic Society 24, 1233 (2004).
11. K. Park, I.H. Han, Materials Science and Engineering B119, 55 (2005).
12. J.Z. Jiang, G.F. Goya, H.R. Rechenberg, J. Phys.: Condens. Mater 11, 4063 (1999).
13. G.F. Goya, H.R. Rechenberg, J.Z. Jiang, Journal of Magnetism and Magnetic Materials 218, 221 (2000).
14. C.R. Alves, R. Aquino, M.H. Sousa, H.R. Rechenberg, G.F. Goya, F.A. Tourinho, J. Depeyrot, Journal of Metastable and Nanocrystalline Materials 20-21, 694 (2004).
15. Kameoka Satoshi, Tanabe Toyokazu, Tsai An, Catalyst Letters, Vol. 100, No. 1-2, pp. 89-93, 2005.
16. W.F. Shangguan, Y. Ternaoka, S. Kagawa, Applied catalysis Part B, Vol. 16, No.2, pp. 149-154, 1998.
17. R.C. Wu, H.H. Qu, H. He. Y.B. Yu, Applied Catalysis Part B 48 (1), 49 (2004).
18. Anonymous, Phase diagram for Ceramists, ASTM.
19. G.F. Goya, H.R. Rechenberg, Journal of Applied Physics 84 (2), 1101 (1998).